



CHORUS

This is the accepted manuscript made available via CHORUS. The article has been published as:

Ultrafast Structural Dynamics of Nanoparticles in Intense Laser Fields

Toshiyuki Nishiyama *et al.*

Phys. Rev. Lett. **123**, 123201 — Published 16 September 2019

DOI: [10.1103/PhysRevLett.123.123201](https://doi.org/10.1103/PhysRevLett.123.123201)

Ultrafast structural dynamics of nanoparticles in intense laser fields

Toshiyuki Nishiyama,^{1,2} Yoshiaki Kumagai,³ Akinobu Niozu,^{1,2} Hironobu Fukuzawa,^{2,3} Koji Motomura,³ Max Bucher,⁴ Yuta Ito,³ Tsukasa Takanashi,³ Kazuki Asa,^{1,2} Yuhiro Sato,^{1,2} Daehyun You,³ Yiwen Li,³ Taishi Ono,³ Edwin Kukk,⁵ Catalin Miron,^{6,7} Liviu Neagu,^{7,8} Carlo Callegari,⁹ Michele Di Fraia,⁹ Giorgio Rossi,¹⁰ Davide E. Galli,¹⁰ Tommaso Pincelli,^{10,11} Alessandro Colombo,¹⁰ Takashi Kameshima,¹² Yasumasa Joti,¹² Takaki Hatsui,² Shigeki Owada,² Tetsuo Katayama,¹² Tadashi Togashi,¹² Kensuke Tono,¹² Makina Yabashi,² Kazuhiro Matsuda,¹ Christoph Bostedt,^{4,13,14,*} Kiyonobu Nagaya,^{1,2,†} and Kiyoshi Ueda^{2,3,‡}

¹*Division of Physics and Astronomy, Kyoto University, Kyoto 606-8501, Japan*

²*RIKEN SPring-8 Center, Sayo, Hyogo 679-5148, Japan*

³*Institute of Multidisciplinary Research for Advanced Materials, Tohoku University, Sendai 980-8577, Japan*

⁴*Chemical Sciences and Engineering Division, Argonne National Laboratory, 9700 S. Cass Avenue, Argonne, IL 60439, United States of America*

⁵*Department of Physics and Astronomy, University of Turku, 20014 Turku, Finland*

⁶*LIDYL, CEA, CNRS, Université Paris-Saclay, CEA Saclay, 91191 Gif-sur-Yvette, France*

⁷*Extreme Light Infrastructure - Nuclear Physics (ELI-NP),*

”Horia Hulubei” National Institute for Physics and Nuclear Engineering, 30 Reactorului Street, RO-077125 Măgurele, Jud. Ilfov, Romania

⁸*National Institute for Laser, Plasma and Radiation Physics,*

409 Atomistilor PO Box MG-36, 077125 Măgurele, Jud. Ilfov, Romania

⁹*Elettra - Sincrotrone Trieste, 34149 Basovizza, Trieste, Italy*

¹⁰*Department of Physics, Università degli Studi di Milano, Via Celoria 16 - 20133 Milano, Italy*

¹¹*Fritz Haber Institute of the Max Planck Society, Faradayweg 4-6, 14195 Berlin, Germany*

¹²*Japan Synchrotron Radiation Research Institute (JASRI), Sayo, Hyogo 679-5198, Japan*

¹³*Paul-Scherrer Institute, CH-5232 Villigen PSI, Switzerland*

¹⁴*LUXS Laboratory for Ultrafast X-ray Sciences, Institute of Chemical Sciences and Engineering, École Polytechnique Fédérale de Lausanne (EPFL), CH-1015 Lausanne, Switzerland*

(Dated: July 11, 2019)

Femtosecond laser pulses have opened new frontiers for the study of ultrafast phase transitions and non-equilibrium states of matter. In this letter, we report on structural dynamics in atomic clusters pumped with intense near-infrared (NIR) pulses into a nanoplasma state. Employing wide-angle scattering with intense femtosecond x-ray pulses from a free-electron laser source, we find that highly excited xenon nanoparticles retain their crystalline bulk structure and density in the inner core long after the driving NIR pulse. The observed emergence of structural disorder in the nanoplasma is consistent with a propagation from the surface to the inner core of the clusters.

When matter is irradiated by an intense femtosecond laser pulse, the rapid energy deposition can trigger new and diverse phenomena including non-thermal melting [1,2], bond-hardening [3], or the creation of dense electron – hole plasma [4]. For all of these ultrafast phase transitions, drastic structural changes are expected to occur, and understanding the competing time scales of the driving mechanisms of excitation and de-excitation in these highly excited systems is of fundamental interest.

Atomic clusters have become a testbed for non-linear light – matter interaction studies [5]. A rare-gas cluster exposed to an intense near-infrared (NIR) laser pulse becomes highly ionized, by multiphoton absorption, and can evolve into a nanoscale plasma, called nanoplasma [6,7], which expands quickly just after formation due to Coulombic or hydrodynamic forces [8]. So far, virtually all information about nanoplasma has been deduced from ion and electron time-of-flight (TOF) measurements. But now, intense femtosecond x-ray pulses from novel free-electron laser (FEL) sources allow imaging the structural

dynamics of highly excited systems down to a few tens of nanometers in size with unprecedented spatial and temporal resolution. Recently, structural changes of laser driven clusters were studied with time-resolved single-shot imaging methods, which give information on temporal evolution of cluster shape [9]. Using the small angle x-ray scattering information, the authors reported ultrafast and non-uniform morphology changes of giant xenon (Xe) clusters in agreement with calculations on hydrogen clusters [10]. These studies gave insight into changes of the averaged density profile in nanoplasma formation induced by intense laser field, showing that the nanoplasma expansion is initiated by rapid surface softening. However, the question on the local atomic order in the cluster core during nanoplasma formation remains.

Following the local atomic order with Bragg scattering experiments has been pivotal to understanding ultrafast light-induced phase transitions [1–4, 11–13]. For nanoplasma, a recent time-resolved x-ray pump / x-ray probe wide angle x-ray scattering (WAXS) study observed Bragg reflections shifting to larger momentum

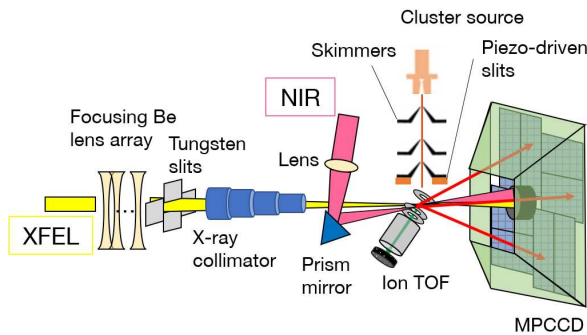


FIG. 1. Experimental setup. The x-ray pulses are focused with Be lenses [16] onto a multiple skimmed jet of Xe clusters and their WAXS patterns are recorded with a MPCCD detector. NIR pulses are overlapped in the interaction region in a close to collinear geometry with a prism mirror and pump the clusters into a nanoplasma state. Ion TOF spectroscopy is used to determine the temporal overlap between the two lasers.

transfer and thus, suggesting lattice contraction of Xe nanocrystals induced within femtoseconds by the first x-ray free-electron laser (XFEL) pulse [12]. The lattice contraction was attributed to the sudden change in the potential energy landscape upon core-level ionization and decay. Intense optical fields, however, dominantly couple to the valence electrons and therefore they are anticipated to induce different dynamics.

In this paper we report on ultrafast Bragg scattering experiments on Xe clusters in intense NIR laser fields. We find that the lattice order survives significantly longer than the 30-femtosecond driving NIR pulse. From the detailed analysis of the Bragg reflections we can deduce that the crystalline core radius shrinks while maintaining the initial crystalline structure. Comparing the nanoplasma core data to the plasma parameters indicates that the observed dynamics are governed by plasma speed of sound.

Our NIR pump / x-ray probe experiments were carried out at the SPring-8 Angstrom Compact Free Electron Laser (SACLA) [14]. A sketch of the experiment is shown in Fig. 1 and in short, a jet of free Xe clusters was irradiated by a single NIR laser pulse followed, at selected delays, by single XFEL pulses. The cluster jet was generated by an adiabatic expansion of Xe gas through a convergent-divergent nozzle with a $200 \mu\text{m}$ diameter and a half-angle of 4° at a stagnation pressure of 30 bar and nozzle temperature of 290 K. The average cluster size was estimated to be around 1×10^7 atoms/cluster by Hagen's scaling law [15]. The cluster jet passed through two skimmers (0.5 mm and 2 mm) and was finally tailored with piezo-driven slits so that its size in the direction of the laser pulses was smaller than the Rayleigh length of the laser pulses.

The NIR laser pulses with a wavelength of 800 nm and pulse length of 30 femtoseconds (fs) were focused with a

single plano-convex lens ($f=500\text{mm}$) and overlapped with the XFEL pulses with a prism mirror at an angle of 3° . A spot size of $(4 \times 10^1) \times (4 \times 10^1) \mu\text{m}^2$ was given for that of the NIR laser at the reaction point. The pulse energy of the NIR laser was adjusted to get an intensity of $4 \times 10^{16} \text{ W/cm}^2$. The XFEL pulses had a wavelength (λ) of 1.1 \AA and pulse duration of 10 fs (FWHM). They were focused with Be lenses to a spot size of $1.4 \times 1.6 \mu\text{m}^2$, significantly smaller than the NIR focus, resulting in an intensity of $4 \times 10^{17} \text{ W/cm}^2$. Spatial and temporal overlap between XFEL and NIR pulses was determined through measuring time-of-flight (TOF) spectra of the clusters. The delay time of the NIR pulse relative to the XFEL pulse was controlled by optical delay system in the range of -500 fs to +2000 fs. The positive delay corresponds to NIR laser arriving early and XFEL late. The temporal jitter between arrival time of XFEL and NIR pulses was measured with the arrival time monitor with 20 fs precision [17].

The scattered x-ray photons were recorded with a multi-port charge-coupled device (MPCCD) octal sensor [18] installed 100 mm downstream from the reaction point. An Al-coated stainless-steel baffle was installed to reduce stray light and fluorescence from the chamber. The detector was also protected with a Kapton foil of $75\text{-}\mu\text{m}$ thickness. The NIR and x-ray pulses were dumped into a three-layer beam stop consisting of C, Al and W sandwich structure. In our setup the observable range of momentum transfer, $q = (4\pi/\lambda) \sin \theta$, was $1.4 - 3.4 \text{ \AA}^{-1}$, corresponding to $2\theta = 14 - 35^\circ$ in scattering angle. Xe ions were detected by the time-of-flight type ion spectrometer [19].

In a first step, static WAXS information was recorded in order to confirm the crystallinity of the nanoparticles. On average we could observe a few Bragg spots for each shot on the detector indicating that we produced a dense target of clusters in the x-ray and NIR focus. Fig. 2 shows the radial average of Bragg spots observed in 638,869 shots. The radial profile has peaks at the positions of reflections from (111), (200) and (220) planes of face-centered cubic (fcc) lattice. Observed fcc structure of Xe clusters agrees well with the structure and lattice constant of bulk Xe [20]. The spots corresponding to hcp (101) Bragg reflection were also observed, and these can be attributed to Xe crystals with randomly stacked close-packed structure [21]. This means that the obtained data include both nearly perfect fcc crystals and nearly randomly stacked crystals. However, the difference of stacking has no effects on the profiles of intense Bragg spots that appear at the fcc (111) reflection region ($q \sim 1.79 \text{ \AA}^{-1}$) [21]. Considering the above facts, the present analysis focuses on the spots observed at $q \sim 1.79 \text{ \AA}^{-1}$.

In the inset of Fig. 2 the hit rate, defined as the number of detected Bragg spots normalized to the number of XFEL shots, for fcc (111) is plotted as a function of delay time. The decrease of the hit rate indicates the

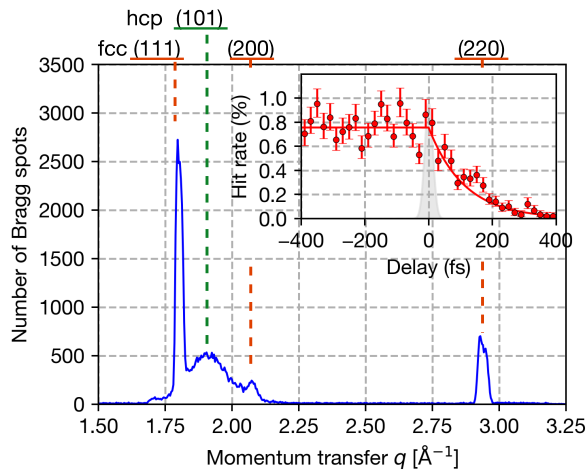


FIG. 2. Radial average of the observed Bragg spots for unpumped clusters. Bragg reflections at the positions of (111), (200) and (220) planes of the fcc lattice are detected. The inset shows the decrease in hit-rate as a function of the delay time for pumped clusters. The data points shown in the inset were derived by averaging the whole data in each delay point.

progressive reduction of coherent diffraction during the nanoplasma formation but it is noteworthy that the fcc crystal structure of Xe clusters survives for several hundred fs after laser irradiation. We also point out that the momentum transfer of (111) Bragg reflection spots did not change within the experimental error ($\pm 0.01 \text{ \AA}^{-1}$). This observation suggests that change of the lattice constant of the Xe fcc crystal is negligible. A recent time-resolved x-ray pump / x-ray probe wide angle x-ray scattering (WAXS) observed Bragg reflections shifting to larger momentum transfer in the excited nanoparticles, indicating the occurrence of lattice contraction of Xe nanocrystals within femtoseconds from the 10-fs hard x-ray pump pulse [12]. The lattice contraction was explained as a consequence of the sudden change in the potential energy landscape upon core-level ionization and decay. Our present results, as obtained with an intense optical pump field, show a different nanoparticle behavior: diffracting volume reduction, but no lattice contraction. The largest excitation cross sections for intense NIR pulses are valence excitation and inverse Bremsstrahlung heating [6], whilst x-rays excite primarily core electrons. We therefore speculate that the density profile of the nanoparticle excitation is quite different in the two experiments and that the observed structural evolution of the nanoparticles does reflect such different excitation regimes. At present we are unable to make a fully qualified statement in this matter, which will need theoretical support describing the complex and correlated electron and nuclear dynamics.

Before delving into a detailed analysis of the Bragg spots the signal generation shall be briefly discussed. Su-

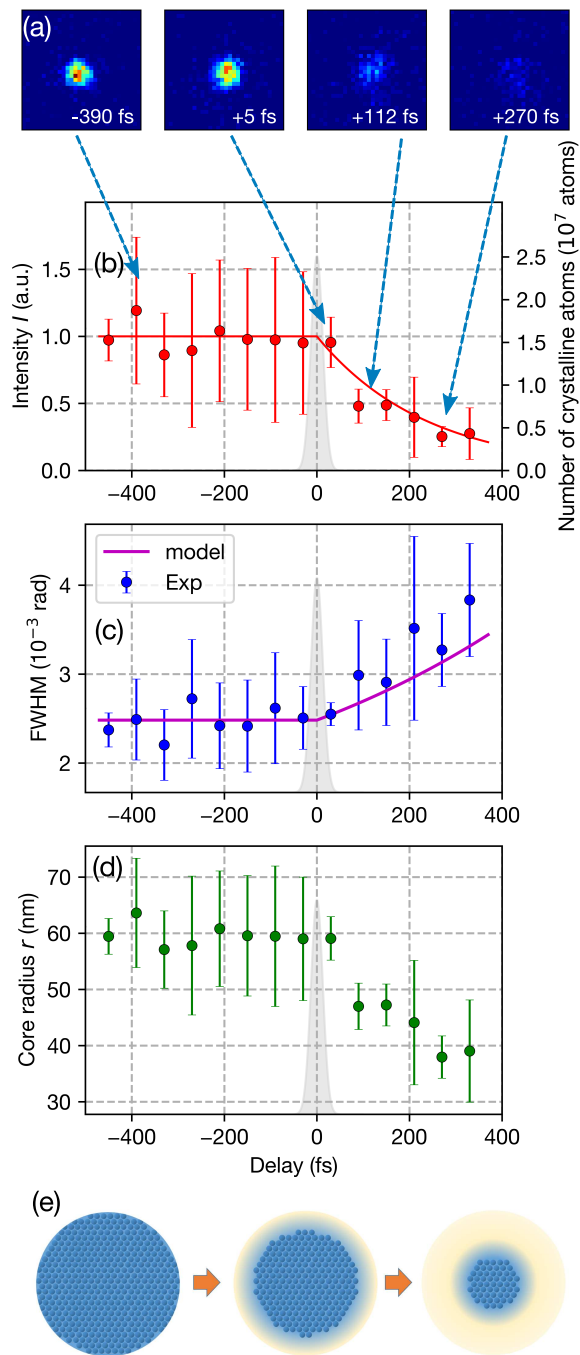


FIG. 3. Delay dependence of profiles of Bragg spots from (111) plane at the NIR power of $4 \times 10^{16} \text{ Wcm}^{-2}$. (a) Characteristic spot images. (b) Temporal evolution of the spot intensity (markers) was fitted by an exponential function (solid red line). Its decay constant was estimated to be around 200 fs. (c) Temporal evolution of the spot width (markers) was compared with surface melting model (solid magenta line). (d) The temporal evolution of the core radius calculated with the experimental (markers) and fitting (solid red line in (b)) data. The error bars of (b), (c) and (d) show standard deviations. (e) A scheme of cluster disordering that proceeds from the surface and is consistent with our experiments.

personic jet expansion always leads to a distribution in cluster sizes [15]. Further, the x-ray scattering signal is convoluted with the focal volume intensity distribution [22]. In order to create a reliable data set we therefore only considered the 5 % most intense signals at each delay point, i.e., only the signal from the largest clusters in the hottest part of the x-ray focal volume.

To obtain information on the local structural changes in Xe clusters, we carried out a profile analysis of Bragg spots. According to the x-ray scattering theory, the Bragg spot intensity is related to the crystal volume, the photon density, and the random displacement of atoms in crystal (the Debye-Waller factor). The spot width is related to the particle size and strain of crystal. We estimated the intensity, which is the product of the area and the height of Bragg spot, and width of each Bragg spot by fitting with a 2D Gaussian function. In Fig. 3 (a) we show the characteristic spots from fcc (111) reflection at various delay times. Fig. 3 (b) and (c) show the temporal evolution of fitted intensity and width of the fcc (111) Bragg spots. The data show that the intensity of Bragg spots was weakened upon NIR irradiation (Fig. 3 (b)), which is consistent with the decrease of the hit rate. At the same time, the spot width increased (Fig. 3 (c)), and the increase reached a few tens percent.

The simultaneous decrease in intensity and increase in Bragg spot width indicates that the crystal volume decreases [23] or in other words, a non-uniform process for crystal disordering. A uniform random displacement of the atoms in the crystal, represented with the Debye-Waller approximation, would not affect the spot width. To substantiate this interpretation we performed Bragg scattering calculations on a simplified model (see the supplemental material in detail). In our model we assumed three principal disordering mechanisms: a random disorder, a core disorder, and a surface disorder. The results show that the surface disorder is in best agreement with the experimental observations and our interpretation of the Debye-Waller factor.

For further insight into the NIR induced dynamics we performed a consistency check of the spot intensity and spot width data. In a first step, we started with a simple model assuming that the decrease of the spot intensity is proportional to the crystal volume and the time-dependent signal is reflecting the volume decrease. For spherical fcc Xe clusters, the crystal radius is then related to the spot intensity as follows:

$$r(t) = \begin{cases} r_0 & (t < 0) \\ r_0 \left(\frac{I(t)}{I_0} \right)^{1/3} & (t > 0) \end{cases} \quad (1)$$

Here r_0 is the radius of cluster in the neutral state (60 nm), I_0 is the intensity of Bragg spot from pristine clusters, $r(t)$ and $I(t)$ are cluster radius and intensity of Bragg spot at the delay time t , respectively. In a second step we calculate the resulting spot width with the

Scherrer equation [24], which relates the FWHM of Bragg spot β and the size of nanoscale crystal as follows:

$$\beta(t) = \frac{2\lambda}{3r(t) \cos \theta}. \quad (2)$$

Here λ is the wavelength of the incident photons, and θ is the Bragg angle. Note that the original formula is in terms of a generalized length scale equal to the cube root of the particle volume. The resulting Bragg peak width from this purely spot intensity based model are added to the measured spot width data Fig. 3 (c) as a solid magenta line. The modeled and measured spot width agree well, showing that the spot intensity reduction and spot width increase are correlated. The data shows that the superheated clusters lose crystalline order from their surface with an ever shrinking crystal core. The process is depicted in Fig. 3 (e).

From the data and with Eq. (2) the average radius of the crystalline particle core as a function of delay can be inferred, which is shown in Fig. 3 (d). The core radius of the undisturbed clusters is stable around 60 nm but upon NIR excitation the crystalline core radius shrinks rapidly. This result is qualitatively similar to an earlier ultrafast imaging experiment which is sensitive to the envelope of the particle [9]. This previous experiment revealed that the nanoplasma expansion proceeds via a developing density gradient at the nanoparticle surface akin to non-thermal surface melting but no information about the inner structure could be obtained. Our data show that the cluster core in the nanoplasma maintains a crystalline bulk-like structure long after the NIR pump pulse is over, but the crystalline fraction is reduced over time (hereafter defined shrinkage). From Fig. 3 (d) and our model we can estimate that the core shrinks with a speed of 7×10^4 m/s.

We can discuss our results in light of previous studies about non-linear NIR laser – cluster interactions and nanoplasma formation [5–7]. At the early stage of laser – cluster interaction, many electrons are photo-ejected and the nanoscale cluster becomes positively charged. Electrons subsequently released are confined by the developing Coulomb potential, leading to the formation of a non-equilibrium nanoplasma. During the laser irradiation, electrons gain energy from the laser field and the cluster is heated via inverse Bremsstrahlung processes. The nanoplasma expands into vacuum due to internal pressure of the electron gas as well as the Coulomb forces. In general, for small clusters the expansion is dictated by Coulombic interaction and for large clusters by hydrodynamic expansion [5,6,25]. In our case of very large clusters, hydrodynamic expansion with the plasma speed of sound is predicted [6,22,26].

To estimate the relevant plasma parameters, we measured the NIR laser produced ion kinetic energy distribution with a time-of-flight spectrometer in a reference measurement, similar to previous studies [6,22,26]. Fitting

the ion spectra, we estimated an average charge state Z of 30 from the time-of-flight data and a resulting electron density n_e of $4 \times 10^{23}/\text{cm}^3$. Using the experimentally determined Z and n_e in full plasma simulations with FLYCHK [27] we infer an electron temperature T_e of ~ 300 eV and an electron-ion equilibrium time τ_{e-i} [8] of ~ 350 fs. The resulting plasma speed of sound, described as $\sqrt{Zk_B T_e / M}$ (k_B is the Boltzmann constant and M is the atomic mass of Xe), is on the order of 8×10^4 m/s.

Most interestingly, the plasma speed of sound determines the speed of hydrodynamic expansion, and the numeric value above comes remarkably close to our measured core shrinking speed (7×10^4 m/s). While so far the interior dynamics of the non-equilibrium nanoplasmas remained elusive, our data can connect previous imaging studies on surface dynamics [9] to the dynamics in the nanoparticle core. The imaging studies [9] showed an expansion from the surface, and our results show a continuous shrinking of the crystalline volume in the core. Connecting the two data sets of surface expansion/softening (exterior dynamics) to the core shrinking and related loss of crystalline order from the surface (interior dynamics) we conclude that the disordering starts on the surface and propagates to the interior with a speed be compatible with the plasma speed of sound. This interpretation is compatible with ion time of flight studies on shell expansion in core-shell structures [28,29] and theoretical modeling of laser-driven hydrogen clusters [10]. In particular, the experimentally determined core shrinking speed is in good agreement with a theoretical study on the expansion dynamics of hydrogen nanoplasma in intense laser fields by Peltz et al. [10] but here we can go one step further. Our data show that even in the highly excited non-equilibrium state, the nanoplasma core retains its crystalline bulk structure and density beyond the initially driving NIR pulse and even beyond τ_{e-i} . Our interpretation is that the local disordering in nanoplasma proceeds from the surface towards the core, initially protecting the core structure and retaining the bulk lattice configuration until the surface disordering has propagated into the core. For a full understanding of the complex laser-induced dynamics, theoretical studies including the full ionization processes and plasma dynamics [10,30] will need to be performed and compared to our data set.

In summary, we investigated ultrafast and atomic-scale structural changes in nanoplasma with time-resolved WAXS experiments. We revealed that the crystalline order in a Xe cluster to nanoplasma transition is maintained long after the driving laser pulse is over. Based on our diffraction data in conjunction with previous studies we conclude that the local disordering in nanoplasma proceeds from the surface to the core with a speed compatible with the plasma speed of sound. Our findings provide new insight into the structural dynamics of highly non-equilibrium nanoplasma states, their formation and their evolution.

We express our profound gratitude to our deceased colleague, professor Makoto Yao for his invaluable support and help with this study. The XFEL experiments were performed at the BL3 of SACLA with the approval of the Japan Synchrotron Radiation Research Institute (JASRI) and the program review committee (2016A8057, 2016B8077). This study was supported by the X-ray Free Electron Laser Utilization Research Project and the X-ray Free Electron Laser Priority Strategy Program of the MEXT, the Proposal Program of SACLA Experimental Instruments of RIKEN, by JSPS KAKENHI Grant No. 15K17487, by JSPS and CNR under the Japan-Italy Research Cooperative Program, and by the IMRAM project. T.N. acknowledges support from the Research Program for Next Generation Young Scientists of "Dynamic Alliance for Open Innovation Bridging Human, Environment and Materials" in "Network Joint Research Center for Materials and Devices". H.F., K.U. and K.N. acknowledge support from the Research Program of "Dynamic Alliance for Open Innovation Bridging Human, Environment and Materials" in "Network Joint Research Center for Materials and Devices". C.B. and M.B. acknowledge support from the U.S. Department of Energy, Office of Basic Energy Sciences, Division of Chemical Sciences, Geosciences, and Biosciences through Argonne National Laboratory. Argonne is a U.S. Department of Energy laboratory managed by UChicago Argonne, LLC, under contract DE-AC02-06CH11357. G.R., D.E.G, T.P. and A.C. acknowledge support from NOXSS PRIN contract of MIUR, Italy. M.D.F. and C.C. acknowledge support from the "Japan-Italy Research Cooperative Program".

* Christoph Bostedt: christoph.bostedt@psi.ch

† Kiyonobu Nagaya: nagaya@scphys.kyoto-u.ac.jp

‡ Kiyoshi Ueda: ueda@tagen.tohoku.ac.jp

- [1] C. W. Siders, A. Cavalleri, K. Sokolowski-Tinten, C. Tóth, T. Guo, M. Kammler, M. H. von Hoegen, K. R. Wilson, D. von der Linde, and C. P. J. Barty, *Science* **286**, 1340 (1999).
- [2] G. Sciaini, M. Harb, S. G. Kruglik, T. Payer, C. T. Hebeisen, F. J. M. zu Heringdorf, M. Yamaguchi, M. H. von Hoegen, R. Ernstorfer, and R. J. D. Miller, *Nature* **458**, 56 (2009).
- [3] R. Ernstorfer, M. Harb, C. T. Hebeisen, G. Sciaini, T. Dartigalongue, and R. J. D. Miller, *Science* **323**, 1033 (2009).
- [4] L. B. Fletcher, H. J. Lee, T. Döppner, E. Galtier, B. Nagler, *et al.*, *Nat. Photon.* **9**, 274 (2015).
- [5] T. Fennel, K.-H. Meiwes-Broer, J. Tiggesbäumker, P.-G. Reinhard, P. M. Dinh, and E. Suraud, *Rev. Mod. Phys.* **82**, 1793 (2010).
- [6] T. Ditmire, T. Donnelly, A. M. Rubenchik, R. W. Falcone, and M. D. Perry, *Phys. Rev. A* **53**, 3379 (1996).
- [7] T. Ditmire, J. W. G. Tisch, E. Springate, M. B. Ma-

- son, N. Hay, R. A. Smith, J. Marangos, and M. H. R. Hutchinson, *Nature* **386**, 54 (1997).
- [8] V. P. Krainov and M. B. Smirnov, *Phys. Rep.* **370**, 237 (2002).
- [9] T. Gorkhover, S. Schorb, R. Coffee, M. Adolph, L. Foucar, *et al.*, *Nat. Photon.* **10**, 93 (2016).
- [10] C. Peltz, C. Varin, T. Brabec, and T. Fennel, *Phys. Rev. Lett.* **113**, 133401 (2014).
- [11] A. M. Lindenberg, J. Larsson, K. Sokolowski-Tinten, K. J. Gaffney, C. Blome, *et al.*, *Science* **308**, 392 (2005).
- [12] K. R. Ferguson, M. Bucher, T. Gorkhover, S. Boutet, H. Fukuzawa, *et al.*, *Sci. Adv.* **2**, e1500837 (2016).
- [13] I. Inoue, Y. Inubushi, T. Sato, K. Tono, T. Katayama, *et al.*, *Proc. Natl. Acad. Sci. USA* **113**, 1492 (2016).
- [14] K. Tono, T. Togashi, Y. Inubushi, T. Sato, T. Katayama, *et al.*, *New J. Phys.* **15**, 083035 (2013).
- [15] O. F. Hagen, *Rev. Sci. Instrum.* **63**, 2374 (1992).
- [16] T. Katayama, T. Hirano, Y. Morioka, Y. Sano, T. Osaka, S. Owada, T. Togashi, and M. Yabashi, *J. Synchrotron Rad.* **26**, 333 (2019).
- [17] T. Katayama, S. Owada, T. Togashi, K. Ogawa, P. Karvinen, *et al.*, *Struct. Dyn.* **3**, 034301 (2016).
- [18] T. Kameshima, S. Ono, T. Kudo, K. Ozaki, Y. Kirihara, *et al.*, *Rev. Sci. Instrum.* **85**, 033110 (2014).
- [19] H. Fukuzawa, K. Nagaya, and K. Ueda, *Nucl. Instrum. Methods Phys. Res. A* **907**, 116 (2018).
- [20] D. R. Sears and H. P. Klug, *J. Chem. Phys.* **37**, 3002 (1962).
- [21] P. N. Pusey, W. van Meegen, P. Bartlett, B. J. Ackerson, J. G. Rarity, and S. M. Underwood, *Phys. Rev. Lett.* **63**, 2753 (1989).
- [22] T. Gorkhover, M. Adolph, D. Rupp, S. Schorb, S. W. Epp, *et al.*, *Phys. Rev. Lett.* **108**, 245005 (2012).
- [23] J. Als-Nielsen and D. McMorrow, in *Elements of Modern X-ray Physics* (Wiley, 2011) Section 5.4, 2nd ed.
- [24] A. Patterson, *Phys. Rev.* **56**, 978 (1939).
- [25] S. P. Hau-Riege, R. A. London, and A. Szoke, *Phys. Rev. E* **69**, 051906 (2004).
- [26] D. D. Hickstein, F. Dollar, J. A. Gaffney, M. E. Foord, G. M. Petrov, *et al.*, *Phys. Rev. Lett.* **112**, 115004 (2014).
- [27] H. K. Chung, M. H. Chen, W. L. Morgan, Y. Ralchenko, and R. Lee, *High Ener. Dens. Phys.* **1**, 3 (2005).
- [28] M. Hoener, C. Bostedt, T. H. L. Landt, E. Eremina, H. Wabnitz, T. Laarmann, R. Treusch, A. R. B. de Castro, and T. Möller, *J. Phys. B: At. Mol. Opt. Phys.* **41**, 181001 (2008).
- [29] C. Bostedt, M. Adolph, E. Eremina, M. Hoener, D. Rupp, S. Schorb, H. Thomas, A. R. B. de Castro, and T. Möller, *J. Phys. B: At. Mol. Opt. Phys.* **43**, 194011 (2010).
- [30] P. J. Ho, C. Knight, M. Tegze, G. Faigel, C. Bostedt, and L. Young, *Phys. Rev. A* **94**, 063823 (2016).